JOM, Vol. 68, No. 9, 2016
DOI: 10.1007/s11837-016-2017-8

Effect of TiO_2 Content on the Crystallization Behavior of Titanium-Bearing Blast Furnace Slag

MEILONG HU,[1,2] RUIRUI WEI,[1] FANGQING YIN,[1] LU LIU,[1] and QINGYU DENG[1]

1.—College of Materials Science and Engineering, Chongqing University, No. 174, Shazheng Street, Chongqing 400044, China. 2.—e-mail: hml@cqu.edu.cn

The content of TiO_2 has an important influence on both the basic structure and the crystallization behavior of titanium-bearing blast furnace (BF) slag. The results of thermodynamic calculations show that, when the mass content of TiO_2 is smaller than 25%, $CaTiO_3$ increases as the content of TiO_2 increases. However, when the TiO_2 content is more than 25%, the $CaTiO_3$ content decreases and TiO_2 gradually increases. The results of a confocal laser scanning microscopy (CLSM) experiment show that, when the TiO_2 mass content is 10%, $Ca_2MgSi_2O_7$ and $Ca_2Al_2SiO_7$ are the main crystallized phases resulting from the molten slag. Furthermore, when the TiO_2 mass content is 20%, $CaMgSi_2O_6$, $Ca(Ti,Mg,Al)(Si,Al)_2O_7$ and dendrite $CaTiO_3$ are the crystallized phases, while when the TiO_2 mass content increases to 30%, $CaTiO_3$ is the sole phase. The discrepancy between the CLSM results and the thermodynamic calculations occurs mainly due to the high melting point of the titanium-bearing BF slag. During the cooling process for the molten slag, $CaTiO_3$ is crystallized first, due to its high crystallization temperature. Furthermore, the molten slag is solidified in its entirety before the other phases crystallize.

INTRODUCTION

In China, titanium-bearing blast furnace (BF) slag is a typical by-product produced during the smelting process of iron from iron ores, and contains about 20–30% TiO_2. As such, its chemical and mineral composition is distinct from that of the BF slag produced in other locations. As a result, titanium-bearing BF slag has been collected and stored in open spaces in China because it is both a waste product and difficult to dispose of. For example, 70 million tons of such slag has built up in the Panzhihua-Xichang area since the 1970s, and its volume continues to increase at a rate of 3.5–4.0 million tons per year. This accumulation has aroused widespread concern over both the protection of the environment and the secondary utilization of a valuable resource, specifically titanium. For BF processes in the region, more than 50% of the titanium from the raw ore enters into BF slag, forming the typical titanium-bearing BF slag.

To solve this serious environmental issue caused by the storage of slag, as well as the potential of recycling the titanium-rich resource, much attention has focused on taking full advantage of the titanium-bearing slag. In recent years, investigations have focused on its properties as well as on methods for extracting valuable metals, where the focus has been on acid leaching,[1] alkaline leaching,[2] Ti–Si alloy and Ti–Si-Al alloy preparation,[3,4] TiC preparation,[5] and concentrating titanium in titanium–enriched phases,[6] among others. However, the employment of these methods still contributes to heavy secondary pollution and has a high cost. Therefore, the enrichment behavior of titanium-enriched phases has become a significant emphasis in recycling slag, and the crystallization behavior of titanium-bearing slag becomes more important in the utilization of the secondary titanium resource.

In order to promote the selective enrichment of titanium-enriched phases during the crystallization of titanium-bearing BF slag, the crystallization behavior and crystallization mechanism of the

(Published online July 21, 2016)

Table I. The chemical composition of slag with different amount of TiO_2

Composition (wt.%)						
No.	CaO	SiO_2	MgO	Al_2O_3	TiO_2	$\frac{n(CaO)}{n(SiO_2)}$
1	39.0	39.0	8.0	14.0	0	1.0
2	36.5	36.5	8.0	14.0	5.0	1.0
3	34.0	34.0	8.0	14.0	10.0	1.0
4	31.5	31.5	8.0	14.0	15.0	1.0
5	29.0	29.0	8.0	14.0	20.0	1.0
6	26.5	26.5	8.0	14.0	25.0	1.0
7	24.0	24.0	8.0	14.0	30.0	1.0

titanium phase in such slag become particularly important in order to study the secondary utilization of titanium resources in the slag. Therefore, investigating the crystallization process of this slag is a meaningful endeavor for the comprehensive utilization of resources, especially titanium-enriched phases, and such a study can provide some valuable data for the crystallization of titanium-bearing BF slag and offer the support to control the crystallization process of the slag, and then promote its comprehensive utilization.

Wang et al. have studied a variation of the Ti-enriched phase with the addition of SiO_2 and TiO_2 into titanium-bearing BF slag.[7] Sung et al. investigated the effect of MgO on the crystallization behavior of the $CaO\text{-}Al_2O_3\text{-}MgO$ system,[8] their results indicating that the crystallization temperature increased during isothermal conditions and continuous cooling with a higher MgO content. Further, the shortest incubation time they observed was at a lower MgO content. Handfield et al. determined that small TiO_2 additions can decrease the viscosity of the slag,[9] while large TiO_2 additions had the opposite effect, which indicated that the TiO_2 additions lowered the viscosity by affecting the network of the silicate structure. However, the aluminate structure was relatively unaffected by TiO_2 additions.

Li et al. studied the influence of TiO_2 on the precipitation behavior of Ti-bearing BF slag using a single, hot thermocouple by applying both thermodynamic calculations and kinetic theory.[10] Their results showed that the incubation time of the samples was mainly influenced by the TiO_2 content, and that the incubation time decreased by increasing the TiO_2 content of the samples. For example, the addition of TiO_2 was favorable in the formation of the Ti-enrichment crystals. Conversely, the effect of the TiO_2 content on the crystallization behavior of titanium-bearing BF slag was not discussed in detail in their research.

The specific objectives of this study are to perform an in situ investigation of the effects of the TiO_2 content on the molten, titanium-bearing BF slag on the resulting precipitation, as well as to investigate the dendrite growth of the crystallization phases using confocal laser scanning microscopy (CLSM).

EXPERIMENT AND CHARACTERIZATION

Preparation of the Synthesized Slag

The synthesized slag used in this experiment was prepared by pre-melting 100 g of chemical reagent-grade CaO (98%), MgO (98%), SiO_2 (99%), TiO_2 (99%) and Al_2O_3 (98%) powder mixture with a target composition referred to in the industrial slag composition. Details for preparing synthesized slag followed published procedures.[11]

Observation of the In Situ Slag Crystallization Using CLSM at Different TiO_2 Contents

To study the effects of the TiO_2 content on the crystallization behavior of titanium-bearing slag, the weights of MgO and Al_2O_3 were kept constant and that of TiO_2 was changed from 0% to 30%, at a constant of the basicity of 1.0, for both the thermodynamic calculations and experiments. Table I shows the chemical composition of the slag with varying TiO_2 contents.

Melting and solidification of the synthesized slag samples took place in a platinum crucible, measuring 8 mm in inner diameter and 5 mm in height, and in an argon atmosphere in the CLSM. The slag sample was heated to 1500°C in order to smelt the slag completely, with a heating rate of 300°C/min and held for 2 min, and then cooled rapidly to the target temperature to more strongly confirm the initial crystalline phase, with a cooling rate of 600°C/min, and held for enough time to observe the isothermal crystallization process of the slag. Finally, the slag was cooled to room temperature until no additional crystal growth occurred. The sample temperature was measured by a B-type thermocouple, which was welded to the bottom of the Pt holder. The temperature accuracy of the device was confirmed through melting samples of pure copper, with a melting point of 1083°C, and of

pure nickel, with a melting point of 1453°C. In order to determine the crystallization process during the isothermal process, video recordings of experiment were analyzed. The images captured and digitized from the video were analyzed using ImageJ software.

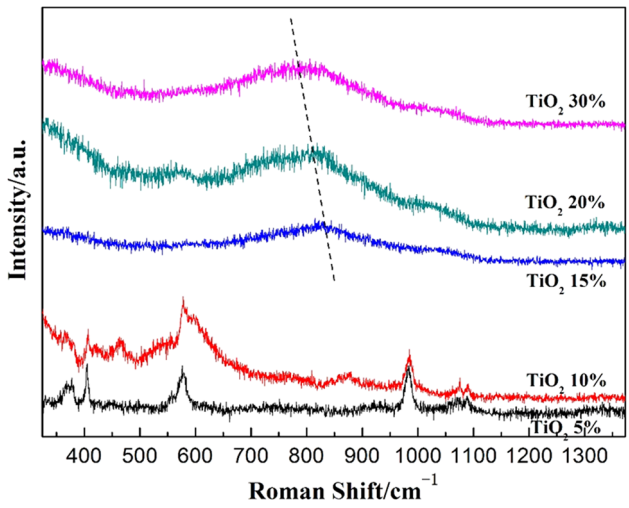

Fig. 1. Raman spectra for samples with different contents of TiO_2 at room temperature.

Characterization

The basic structures of the slag, prepared using a chemical reagent and at varying TiO_2 contents, were characterized by Raman spectroscopy. The cooled samples were crystalized at varying contents of TiO_2, and were characterized by x-ray diffraction (XRD) and scanning electron microscopy (SEM) to confirm the phases and morphologies of the crystals precipitated from the titanium-bearing BF slag.

RESULTS AND DISCUSSION

Effect of the TiO_2 Content on the Basic Structure of the Slag

Results of the effects of the TiO_2 content on the structure of the oxide system have indicated that TiO_2 existed in the system in the form of $[TiO_4]$, and served as a network-former.[12] Silicate networks were more polymerized because of the increase in the TiO_2 content. A significant fraction of Ti^{4+} contributed to the formation of the network and entered the silicate network.[13] To study the effects of TiO_2 content on the structure of the pentabasic system of titanium-bearing BF slag, Raman spectra, with varying TiO_2 content and at room temperature, were completed, as shown in Fig. 1. It was observed that the relative intensity of the Raman signals, at approximately 750–900 cm^{-1}, had a slight shift toward a lower frequency when the TiO_2 content was more than 15 mass%. The main

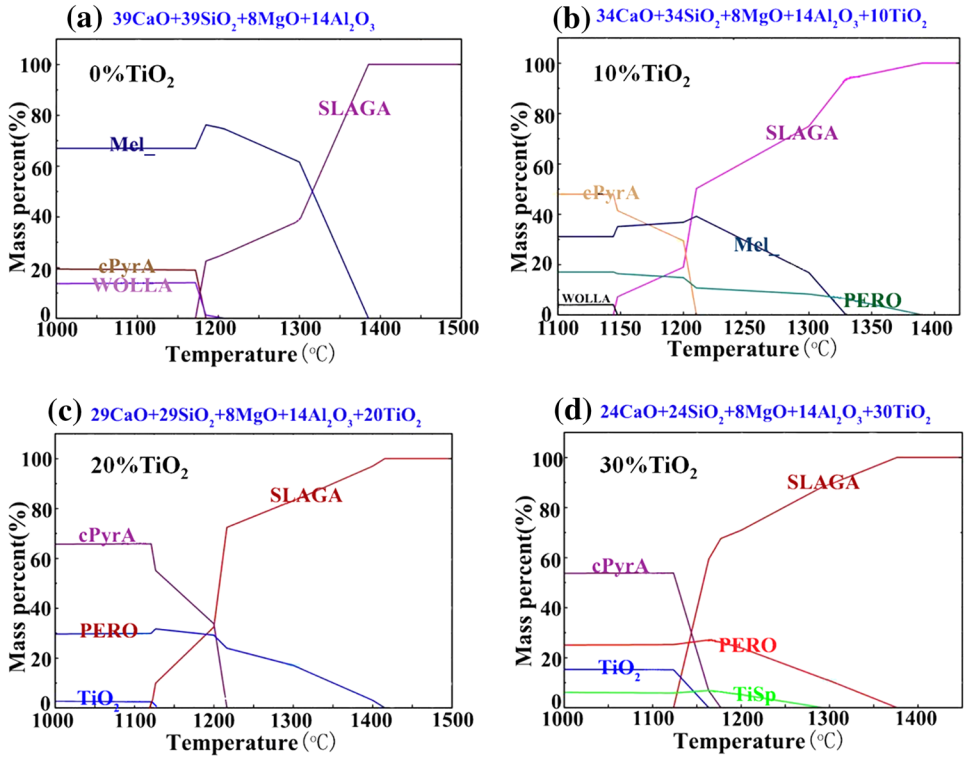

Fig. 2. Theoretical isothermal phase composition of the slag with varying amounts of TiO_2 during cooling: (a) 0% TiO_2, (b) 10% TiO_2, (c) 20% TiO_2, and (d) 30% TiO_2. cPyrA—clinopyroxene, Mel—melilite, SLAGA—slag, PERO—perovskite, TiSp—titan-spinel, WOLLA—wollastonite.

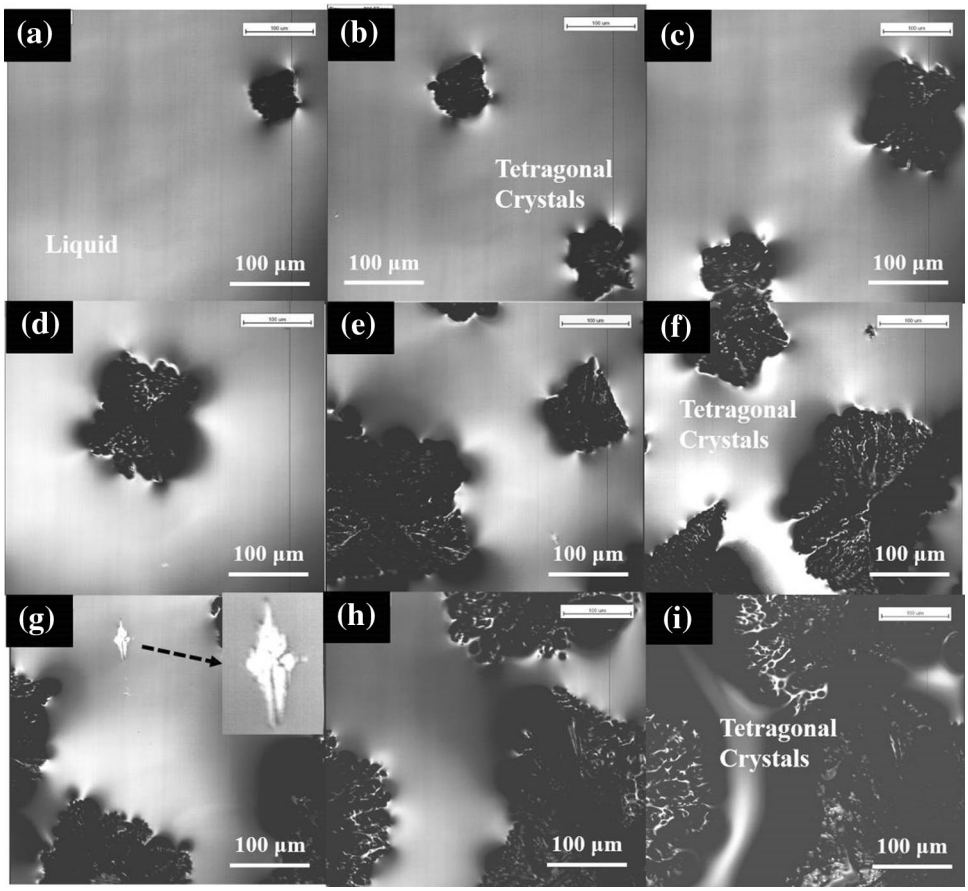

Fig. 3. The crystallization process of the slag with 10% TiO_2 at 1100°C: (a) 800.75 s, (b) 806.57 s, (c) 815.57 s, (d) 824.14 s, (e) 852.66 s, (f) 879.36 s, (g) 919.74 s, (h) 962.56 s, and (i) 1075.51 s.

reason was that some of the network-forming Ti^{4+} was transformed into 6-coordinated network modifiers when the mass fraction of TiO_2 was increased to 15 mass%. The effect of the TiO_2 content on the structure of titanium-bearing slag was small when the TiO_2 content was lower than 10%, due to the presence of free oxygen. It was also demonstrated that the TiO_2 content in the pentabasic, titanium-bearing slag had an influence on the basic structure.

Thermodynamic Calculations

Figure 2 shows the results of thermodynamic calculations at different TiO_2 contents using FactSage software and demonstrates that four phases are generated in the isothermal crystallization process of pentabasic, titanium-bearing BF slag with 10% TiO_2, including $CaTiO_3$, melilite, clinopyroxene, and wollastonite. Owing to the presence of TiO_2, the resulting $CaTiO_3$ generated, and part of the CaO entered into clinopyroxene from melilite, as compared to quarternary slag with no titanium.

Similarly, the four phases generated by the slag with 20% TiO_2 were $CaTiO_3$, titan-spinel, clinopyroxene, and TiO_2. Compared to the slag with 10% TiO_2, wollastonite and melilite disappeared; however, the spinel and TiO_2 emerged within the slag. The same phases were present in the BF slag with 20% TiO_2 and 30% TiO_2. However, the degree of crystallinity of $CaTiO_3$ decreased slightly, while TiO_2 increased.

Thus, as demonstrated, when the basicity of the slag was equal to 1.0, the initial crystallization temperature of the slag initially increased and then decreased with an increase in the TiO_2 content. Further, it approached the peak at the TiO_2 content of 20%. The crystallized products present in the quaternary slag without titanium were mainly melilite and clinopyroxene, with a trace amount of wollastonite. Additionally, if TiO_2 was present in the slag, then $CaTiO_3$ was crystallized first. With an increase in the TiO_2 content, the number of phases containing titanium increased. In addition, the amount of $CaTiO_3$ increased initially and then decreased, while TiO_2 gradually increased. The production of $CaTiO_3$ was the main phase bearing titanium in the slag when the TiO_2 content was equal to 20%, and the crystalline quantity of TiO_2 was equal to the TiO_2 content of 30%.

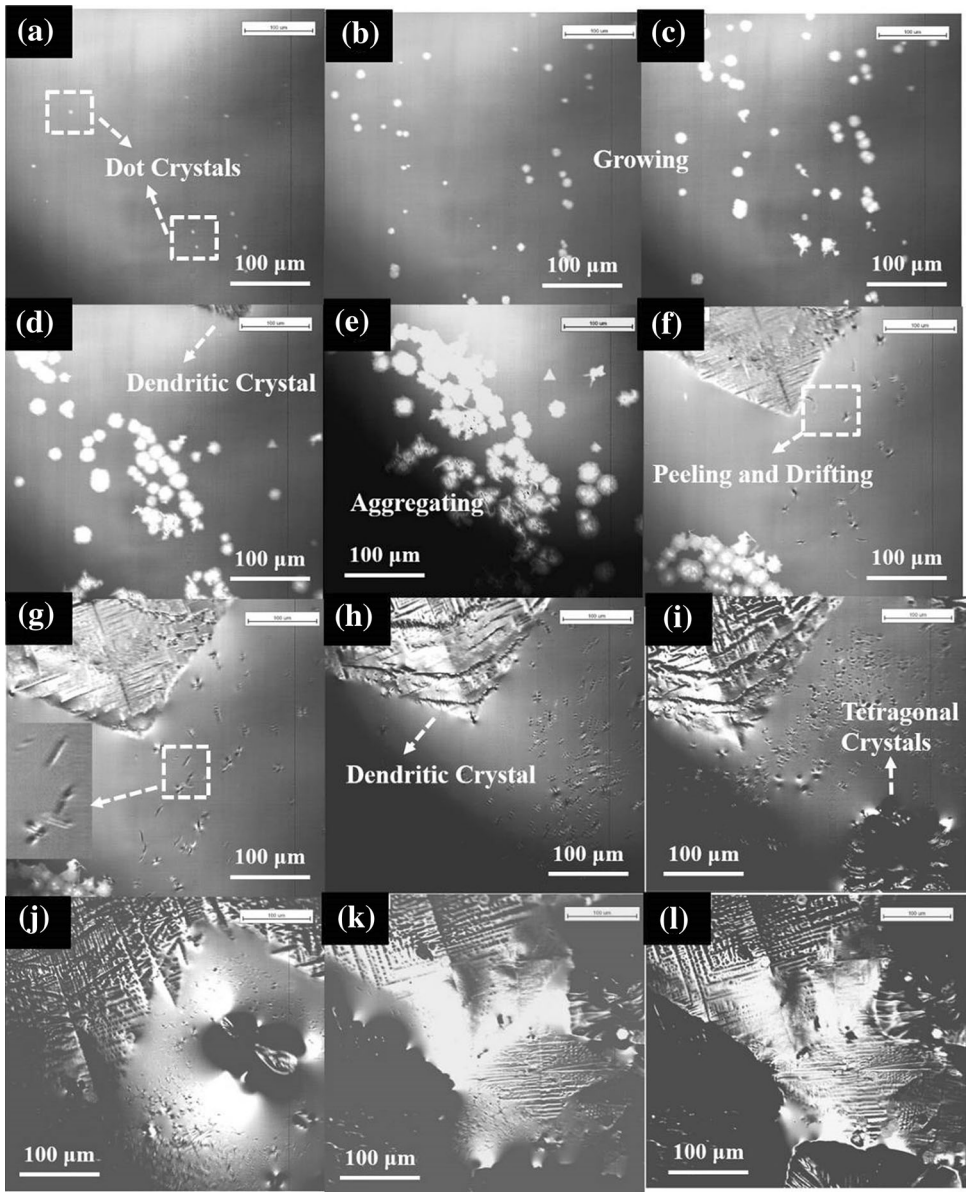

Fig. 4. The crystallization process of the slag with 20% TiO_2 at 1100°C: (a) 657.68 s, (b) 665.87 s, (c) 674.64 s, (d) 686.06 s, (e) 694.29 s, (f) 703.23 s, (g) 710.72 s, (h) 739.57 s, (i) 750.68 s, (j) 769.40 s, (k) 783.41 s, and (l) 790.73 s.

Effects of the TiO_2 Content on the Crystallization of Titanium-Bearing Slag

Figure 3 shows the isothermal crystallization process of pentabasic, titanium-bearing BF slag with 10% TiO_2 using the CLSM method at 1100°C. As illustrated, the initial resulting crystalline phase presented a square-shaped crystal, which grew upward while the liquid phase decreased, and the cooling time increased. The integrated crystallization and the crystal growth process were not observed due to an uncertainty in the initial location of crystallization. The white rhomboidal crystal, as observed in Fig. 3g, occurred during precipitation. This may be the crystal morphology of the square-shaped crystal. According to the resulting crystal morphology of the quaternary BF slag without titanium, it was inferred that the square crystal was melilite.

Figure 4 shows the isothermal crystallization process of the pentabasic titanium-bearing BF slag with 20% TiO_2 using the CLSM method at 1100°C. As shown in Fig. 4a, white dot crystals appeared at the beginning of the crystallization process. As the isothermal crystallization time increased, the white dot crystals grew gradually upward and then transitioned to become irregular, snowy spots, as shown in Fig. 4b–e. Furthermore, dendritic crystals appeared in Fig. 4d. In Fig. 4d–i, it is shown that the dendrite grew slowly.

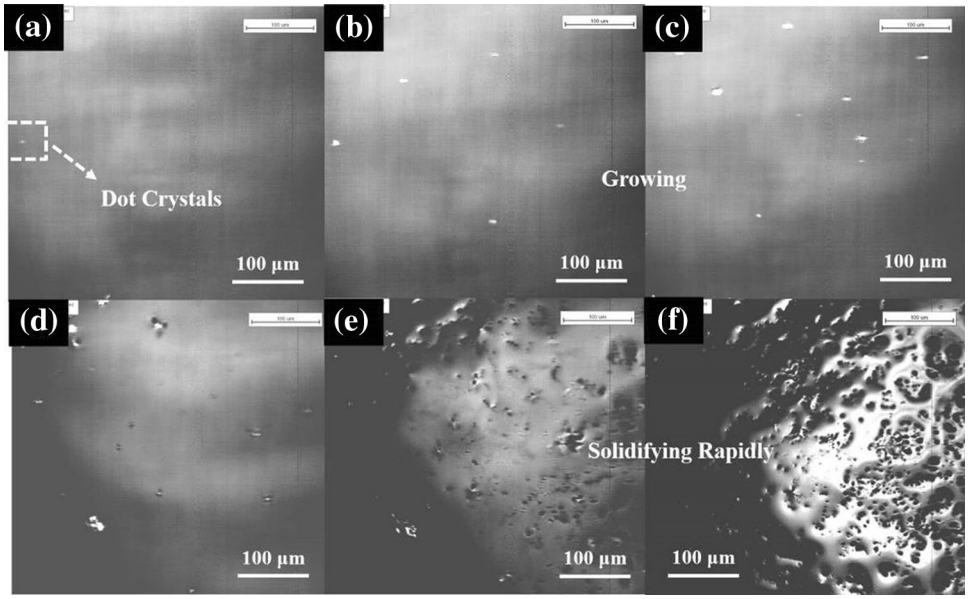

Fig. 5. The crystallization process of the slag with 30% TiO_2 at 1100°C: (a) 654.56 s, (b) 660.18 s, (c) 670.03 s, (d) 687.74 s, (e) 693.26 s, and (f) 695.36 s.

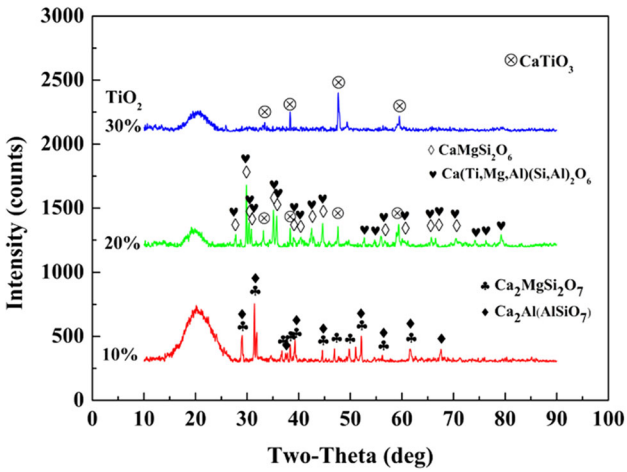

Fig. 6. XRD patterns of slag isothermally crystallized at varying TiO_2 contents.

While the dendrite size experienced little to no significant changes, the thickness of the dendrite increased. Two phenomena were observed from this crystallization process. The first was the gathering or flocculation of the white dot crystals as shown in Fig. 4d–f. This may have been caused by a spontaneous gathering and squeezing out by the dendrite; however, other images appeared to be more of a transition process, where the needle-shaped crystal was constantly peeled from dendrite. Finally, the white dot crystal was attached, as shown in Fig. 4f–h. The needle-shaped crystal may have been the result of the small dendrite peeling from the dendrite during the dendrite growth, while the white dot crystal may have included grains precipitated and not grown upward. Both were from the same phase, indicating that the transition for the small, needle-shaped crystals had occurred. According to the aforementioned speculation, each of the three crystals were $CaTiO_3$. With the further increase in the cooling time, the square-shaped crystal began to crystallize as shown as Fig. 4i.

Figure 5 shows the isothermal crystallization process of pentabasic, titanium-bearing BF slag with 30% TiO_2 using the CLSM method at 1100°C. White dot crystals emerged during the crystallization process of the BF slag, where its crystalline morphology was identical to that of the initial crystalline morphology of the isothermal crystallization process of the slag with 20% TiO_2. From Fig. 5a–d, the crystals grew gradually upward, therefore increasing the crystallization time. When the crystallization process reached a certain time, the slag coagulated completely, as shown in Fig. 5e and f.

Figure 6 shows the XRD results of the BF slag which was isothermally crystallized at the different TiO_2 contents. Furthermore, Figs. 7, 8, and 9 show the SEM images of the surface of the slag. The images indicate that two phases have been generated during the isothermal crystallization process of the pentabasic, titanium-bearing BF slag with 10% TiO_2, including akermanite ($Ca_2MgSi_2O_7$) and gehlenite ($Ca_2Al_2SiO_7$), which both belong to the melilite family. However, these results were inconsistent with the calculation results obtained by the FactSage software. Based on the aforementioned investigation, the crystal belonging to the tetragonal system, appearing more like a square-shaped plate, was identical to the morphology observed with the CLSM. Therefore, the square-shaped crystal observed under the microscope should be classified as melilite. Moreover, the surface of the polished slag had no crystals

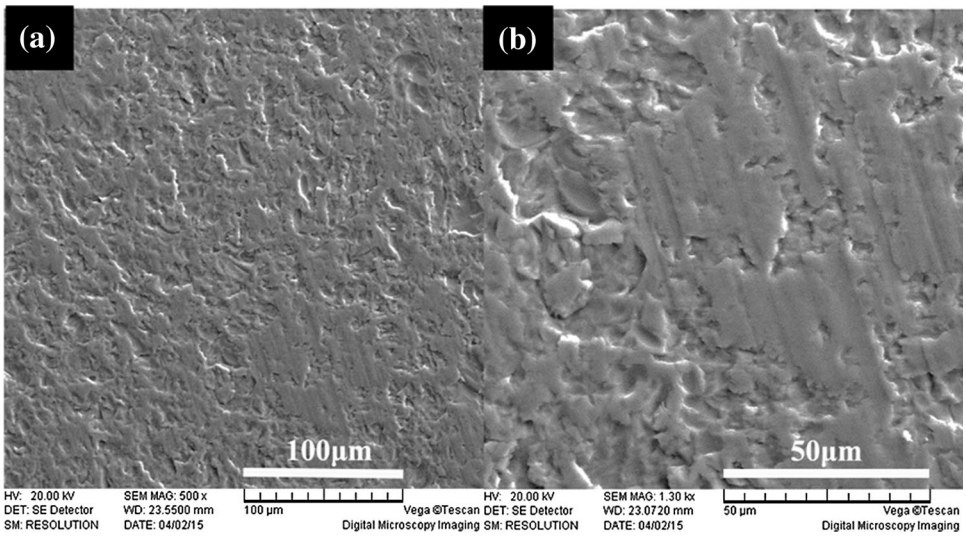

Fig. 7. The SEM images of slag sample surface with 10% TiO_2 after the CLSM experiment: (a) ×500 magnification and (b) ×1300 magnification.

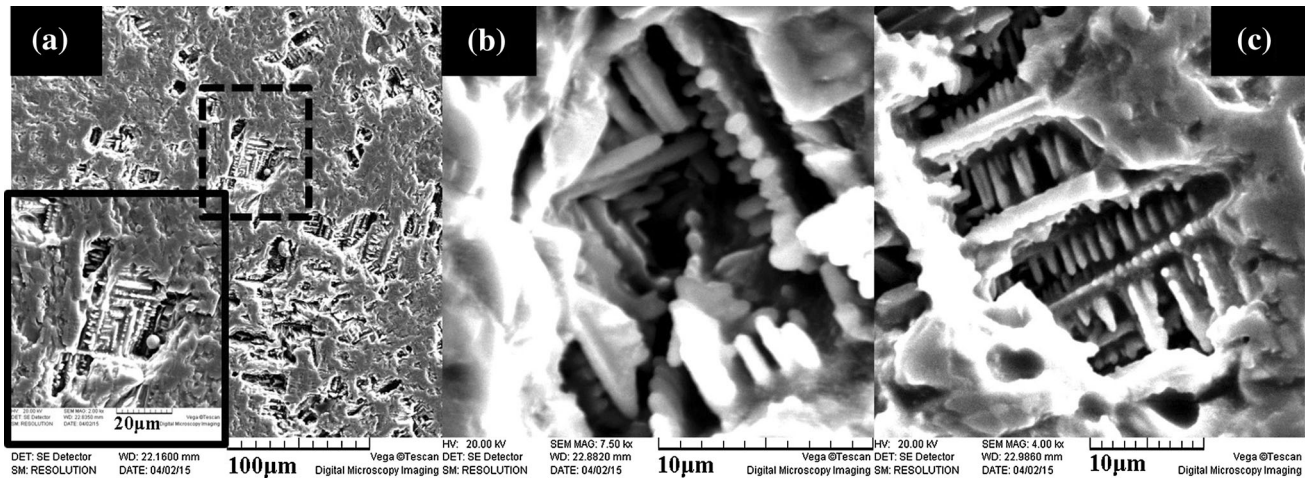

Fig. 8. The SEM images of the slag sample surface with 20% TiO_2 after CLSM experiment: (a) ×2000 magnification, (b) ×7500 magnification and (c) ×4000 magnification.

with the unique morphology, which was characteristic of the melilite and clinopyroxene crystalline phases, as shown in Fig. 7.

Three phases were generated during the isothermal crystallization process of the pentabasic, titanium-bearing BF slag with 20% TiO_2 at 1100°C, two of which were clinopyroxene, including $CaMgSi_2O_6$, and $Ca(Ti,Mg,Al)(Si,Al)_2O_7$, while the other resulting phase was $CaTiO_3$. According to SEM images in Fig. 8, the crystals with the unique morphology were not observed on the surface of the BF slag after polishing. However, dendrite formation was present in the hole, which was projected to be $CaTiO_3$. Therefore, the dendrite observed with the CLSM was likely $CaTiO_3$, while the square-shaped crystal was likely clinopyroxene.

According to the XRD results shown in Fig. 6, $CaTiO_3$ was the unique phase that occurred in the isothermal crystallization process of the pentabasic, titanium-bearing BF slag with 30% TiO_2 using the CLSM method at 1100°C. As shown in Fig. 9, the surface of the slag after polishing was covered by the dendrite, and other compositions of such slag likely formed the amorphous phase.

Numbers 1–7 of the phase diagram shown in Fig. 10 indicate different TiO_2 contents from 0% to 30%, as shown in Table I. As observed in the phase diagram, $CaAl_2Si_2O_8$ was crystallized first when the basicity in the slag maintained a specific basicity of 1.0. Furthermore, CaO reacted with SiO_2 and Al_2O_3 to readily form $CaAl_2Si_2O_8$, rather than when the TiO_2 content was smaller than a basicity of 0.4. Therefore, it was supposed that the activity of CaO in such slag decreased as the TiO_2 content increased. As the CaO content decreased and TiO_2 content increased to more than 0.4, $CaTiO_3$ appeared. Consequently, a higher TiO_2 content proved beneficial to the formation of CaO with

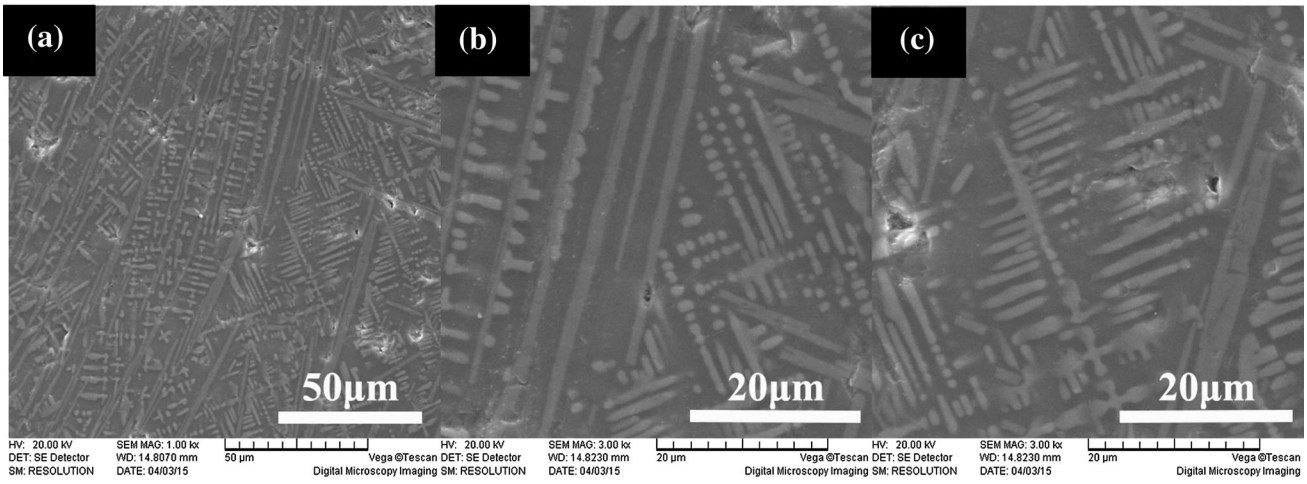

Fig. 9. The SEM images of the slag sample surface with 30% TiO_2 after the CLSM experiment: (a) ×1000 magnification and (b, c) both at ×3000 magnification, but representing different areas.

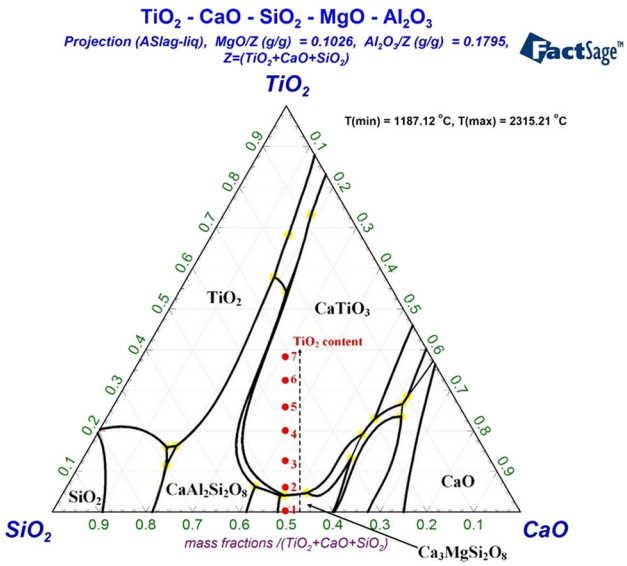

Fig. 10. Diagram from calculations using FactSage of the titanium-bearing BF slag.

Al_2O_3 and SiO_2, while a higher TiO_2 content also resulted in the thermodynamically favorable production of $CaTiO_3$.

The phase diagram calculation results roughly agreed with those of the experiments conducted under super-cooling conditions with a lower TiO_2 content. Specifically, when the cooling rate was much higher, the mixed phases crystallized, for example $CaMgSi_2O_6$ and $Ca(Ti,Mg,Al)(Si,Al)_2O_7$, from the molten slag at a lower TiO_2 content. With an increase in TiO_2, $CaTiO_3$ gradually became the main phase crystallized from the molten slag when the TiO_2 content was higher than basicity of 0.4.

CONCLUSION

In conclusion, combining the experimental results obtained from the isothermal crystallization of quaternary slag without titanium to those of the pentabasic, titanium-bearing BF slag with increasing TiO_2 from 0% to 30%, the primary phase of the BF slag was transformed from a square-shaped melilite to a $CaTiO_3$ dendrite. Melilite was the primary phase of the BF slag during the crystallization process for a TiO_2 content of 0% and 10%. Similarly, TiO_2 was the primary phase for the TiO_2 content of 20%; however, clinopyroxene was also observed. Furthermore, $CaTiO_3$ presented a unique crystalline phase for the TiO_2 content of 30%. Thus, the TiO_2 content in the BF slag proved to have a significant influence on the crystalline phase, crystal morphology, and other characteristics.

This study explains the crystallization process of BF slag with the addition of TiO_2. The results can be used for controlling the crystallization of titanium-rich phases in the slag, promoting the utilization of the titanium-bearing BF slag.

ACKNOWLEDGEMENTS

The authors are especially grateful to Project No. 51404044, supported by the National Natural Science Foundation of China, to Project No. 20130191110015, supported by the Specialized Research Fund for the Doctoral Program of Higher Education of China, and to project supported by Open Foundation of State Key Laboratory of Vanadium and Titanium Resources Comprehensive Utilization of China.

REFERENCES

1. S.-G. Liu, G. Sui, R.A. Cormier, R.M. Leblanc, and B.A. Gregg, *J. Phys. Chem. B* 106, 1307 (2002).
2. B.Z.Z. Zhou and Z. Zhu, *Iron Steel Van. Titan.* 20, 37 (1999).

3. S.X.Z. Li, Z. Li, and Y. Zhou, *J. Chongqing Univ.* 19, 82 (1996).
4. Q. Huang, X. Lv, R. Huang, and J. Song, *Can. Metall. Q.* 52, 413 (2013).
5. Y.Q.H. Li and Z. Yang, *J. Univ. Sci. Technol. Beijing* 18, 231 (1996).
6. X. Lv, Z. Lun, J. Yin, and C. Bai, *ISIJ Int.* 53, 1115 (2013).
7. X. Wang, Y. Mao, X. Liu, and Y. Zhu, *J. Iron Steel Res.* 3, 1 (1990).
8. S.S. Jung and I. Sohn, *Metall. Mater. Trans. B* 43, 1530 (2012).
9. G. Handfiel and G.G. Charette, *Can. Metall. Q.* 10, 235 (1971).
10. J. Li, Z.T. Zhang, L.L. Liu, W.L. Wang, and X.D. Wang, *ISIJ Int.* 53, 1696 (2013).
11. M.L. Hu, L. Liu, X.W. Lv, C.G. Bai, and S.F. Zhang, *Metall. Mater. Trans. B* 45, 76 (2014).
12. Z. Wang, Q.F. Shu, and K.C. Chou, *ISIJ Int.* 51, 1021 (2011).
13. K. Zheng, J.L. Liao, X.D. Wang, and Z.T. Zhang, *J. Non Cryst Solids* 376, 209 (2013).